Journal of Information Hiding and Multimedia Signal Processing ©2019 ISSN 2073-4212
Ubiquitous International Volume **10**, Number **1**, January **2019**

A New Wavelet Threshold Function Based on Gaussian Kernel Function for Image De-noising

Yang Sun[1], Shoulin Yin[1*] and Hang Li[1]

[1]Software College
Shenyang Normal University
Shenyang City, Liaoning Province, 110034, China
*Corresponding author: lihangsoft@163.com

Received March 2018; revised September 2018

Abstract. *Currently, image de-noising has become a hot topic for image classical solution of the estimation problem. The effectiveness of wavelet-based threshold functions for image de-noising is taken into consideration. Therefore, many wavelet threshold functions are proposed to improve the effectiveness of image de-noising, such as hard?threshold, soft threshold and semi-soft threshold function etc,. Nevertheless, these methods are with some demerits including function discontinuity, image edge missing, edge fog, poor smoothness and parameters determined by trial and error. To perfect these shortcomings, a new wavelet threshold function based on Gaussian kernel function is proposed in this paper. First, the existing threshold functions and their problems are introduced. Second, we detailed explain the new threshold function to offset the shortcomings by combining Gaussian kernel function with soft threshold function. Meanwhile, its new properties are proofed. Third, threshold parameter λ is optimized. Finally, experimental results validate that the new method sometimes surpasses recently published leading alternative de-noising methods and achieves a better performance.*
Keywords: Image de-noising, Gaussian kernel function, Wavelet Threshold Function

1. **Introduction.** In the process of image formation, transmission and processing, image can be interfered by noise. Thus the quality of image will decrease. To remove or suppress the noise in image and improve the quality of image, many de-noising methods are generated. Wavelet analysis, a very effective image de-noising method, in time domain and frequency domain has good localization properties and the multi-resolution analysis characteristics [1], it can effectively distinguish useful signal and noise. At present, wavelet de-noising mainly includes three models [2]. 1) Adopting the wavelets singularity detection features to separate signal and noise [3]; 2) Using wavelet coefficient threshold function to reduce the image noise [4]; 3) Bayesian criterion coefficient of wavelet domain method [5] is used for image noise reduction. Where the wavelet threshold shrinkage method is the most widely used in image de-noising due to its simple and effective attribute. The idea of wavelet threshold processing is derived from the Donoho theory [6]. Donoho first gave the general threshold de-noising formula based on orthogonal wavelet transform, it made the complex de-noising problem become easily to solve. However, due to lack of the adaptability of scale space, it is difficult to determine the threshold. The result can lead to fuzzy image edge and poor de-noising performance. So many scholars have put forward different wavelet coefficients scales and their corresponding thresholds to reduce image noise, such as hard threshold [7], soft threshold [8], VisuShrink threshold [9], improved

sub-band adaptive SureShrink threshold [10] and NormalShrink threshold [11]. Although these de-noising algorithms can obtain better de-noising performance, more detail information is eliminated. The image quality is seriously declined, even generating pseudo Gibbs phenomenon. To date, Wang et al. [12] proposed an optimized shape parameter method for image de-noising. Kadhim [13] presented an Particle Swarm Optimization (PSO) algorithm developed to estimate the value of threshold without any priority of knowledge for these distributions. This was done by implementing the PSO algorithm for kurtosis measuring of the residual noise signal to find an optimum threshold value at which the kurtosis function be maximum. Ji et al. [14] employed a de-noising algorithm utilizing wavelet threshold method and exponential adaptive window width-fitting. His method was divided into three parts. First, wavelet threshold method was used to filter the white noise. Second, the data were segmented using data window. Eventually, an exponential fitting algorithm was adopted to fit the attenuation curve of each window, and the data polluted by non-stationary electromagnetic noise were replaced with their fitting results. The above methods have obtained some effect for image de-noising. However, less works aims to improve the threshold function. Therefor, we propose a new wavelet threshold function based on Gaussian kernel function for image de-noising. We optimize wavelet threshold function from two aspects: improving threshold function and shape parameter λ, that significantly improves de-noising and provides clearer implementation compared to state-of-the-art methods. It can be reliably used for de-noising experimental images. Furthermore, new function can enhance the efficiency of image de-noising without the effect of layers number of image decomposition.

The reminder of this paper is organized as follows. Preliminaries are displayed in section 2. Section 3 illustrates the detailed new threshold function and Section 4 presents experimental results. Section 5 concludes this paper.

2. **Preliminaries.**

2.1. **Wavelet threshold function and existing problems.**

Usually, noise is with high frequencies, wavelet threshold de-noising method can deal with threshold for the corresponding wavelet coefficients' high frequency parts, then it reconstructs image and achieves the goal of de-noising. Assuming that image signal with added Gaussian white noise can be described as:

$$f(p,q) = s(p,q) + n(p,q)(p,q = 0,1,2,\cdots,N-1). \tag{1}$$

Where $s(p,q)$ is original image, the mean of $n(p,q)$ is zero. $f(p,q)$ is the noisy image. White Gaussian noisy with variance of δ^2 obeys $N(0,\delta^2)$ distribution. After wavelet transforming, its signal energy mainly focuses on low frequency coefficient. However, the energy of noise mainly distributes in high frequency coefficient. And the coefficient of wavelet decomposition is very small. Principle of threshold de-noising is that it selects appropriate threshold in different scales and makes threshold quantization process for wavelet coefficient. Thereby, the noise is effectively suppressed. Finally, it reconstructs the processed wavelet coefficients and gets the reconstructed de-noising image.

The wavelet threshold de-noising method mainly contains hard and soft threshold de-noising method. Nevertheless, hard threshold function is discontinuous in a certain range. So it may cause some shakeups (such as ringing and Pseudo-Gibbs phenomena etc,.) for the reconstruction signal. Although the soft threshold function is continuous in its domain, there are still some deviations and edge fuzziness phenomenons. To solve the disadvantages of these two methods, semi-soft threshold function [15], interpolation semi-soft threshold function [16] and asymptotic semi-soft threshold function [17] are proposed.

In the above methods, there are still some shortcomings. When $w_{i,j} = \lambda$, $\hat{w}_{i,j}$ is discontinuous in hard threshold function. Though soft threshold function is continuous, there are some deviations between $\hat{w}_{i,j}$ and the wavelet coefficient $w_{i,j}$. When image reconstructing, some details will be lost, image precision will decrease. Using semi-soft threshold function de-noising, SNR of image is improved, but λ_1 and λ_2 are complex. It has little utility. There are spots and deviation in interpolation semi-soft threshold function and asymptotic semi-soft threshold function. Therefore, we propose a new threshold function in this paper.

3. New Wavelet Threshold Method.

3.1. Improved wavelet threshold function.

In order to overcome the shortcomings of the traditional threshold function and based on the principle of Gaussian kernel function. A new threshold function is proposed in this paper described as formula (2), additionally, the optimized λ is explained in 3.2.

$$f(new_x) = \hat{w}_{i,j} = sign(w_{i,j})(|w_{i,j}| - \lambda e^{-\frac{[\alpha((w_{i,j}-\lambda)/\lambda)-\mu]^2}{2\sigma^2}}), |w_{i,j}| > \lambda. \tag{2}$$

Where parameter λ is the representation of threshold. $\hat{w}_{i,j}$ is the representation of estimated wavelet coefficients, $w_{i,j}$ denotes the representation of the wavelet coefficients and $sign(*)$ is the symbolic piecewise function. When $|w_{i,j}| < \lambda$, $f(new_x) = \hat{w}_{i,j} = 0$. On the basis of soft and hard threshold function, α, the shape parameter of the threshold function, is taken between 0 and 1. Due to a complex exponential function (i.e. Gaussian kernel function model) $e^{-\frac{[\alpha((w_{i,j}-\lambda)/\lambda)-\mu]^2}{2\sigma^2}}$ in the improved function, so the new function is more adaptability which is different from other threshold functions. When the value of α is changed, the new function is adjusted flexibly. Figure 1 is the curve with different α in new function, where $\lambda = 0.6$, $\mu = 0$, $\sigma = 1$.

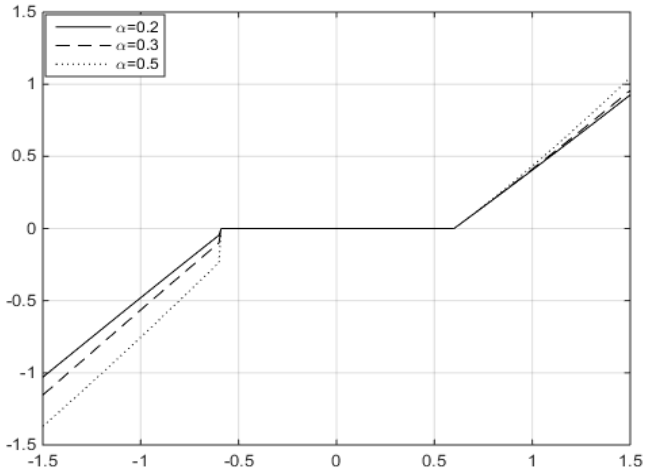

FIGURE 1. New function with different α.

New function is with the following good properties.

Theorem 1. Continuity: there is no break-point, so $f(new_x)$ is a continuous function in its domain.

Remark. From its curve, the domain and its range of the function is $(-\infty, +\infty)$.

Proof. When $x > \lambda$

$$f(new_x) = sign(w_{i,j})(|w_{i,j}| - \lambda e^{-\frac{[\alpha((w_{i,j}-\lambda)/\lambda)-\mu]^2}{2\sigma^2}}). \tag{3}$$

Therefore, right-hand limit of the function is given by:

$$\begin{aligned} \lim f(new_x)_{x\to\lambda^+} &= \lim x_{x\to\lambda^+}(x - \lambda e^{-\frac{[\alpha((w_{i,j}-\lambda)/\lambda)-\mu]^2}{2\sigma^2}}) \\ &= (x - \lambda e^0) \\ &= 0. \end{aligned} \tag{4}$$

When $x < -\lambda$

$$f(new_x) = sign(w_{i,j})(-w_{i,j} - \lambda e^{-\frac{[\alpha((w_{i,j}-\lambda)/\lambda)-\mu]^2}{2\sigma^2}}). \tag{5}$$

Therefore, left-hand limit of the function is abbreviated to:

$$\begin{aligned} \lim f(new_x)_{x\to\lambda^-} &= \lim x_{x\to\lambda^-}(-x - \lambda e^{-\frac{[\alpha((w_{i,j}-\lambda)/\lambda)-\mu]^2}{2\sigma^2}}) \\ &= (-x - \lambda e^0) \\ &= 0. \end{aligned} \tag{6}$$

When $-\lambda \le x \le \lambda$

$$f(new_x) = 0. \tag{7}$$

Considering (5), (6), (7), $\lim f(new_x)_{x\to\lambda^+} = \lim f(new_x)_{x\to\lambda^-} = \lim f(0)$.

Therefore, the new function is a continuous curve in its domain. And it makes up the shortcomings of hard threshold function.

Theorem 2. Monotonicity: $f(new_x)$ is a monofonically increasing function in $(-\infty, +\infty)$, so $f(new_x)$ is an increasing function in its domain.

Proof. When $x > \lambda$

$$f(new_x) = sign(w_{i,j})(x - \lambda e^{-\frac{[\alpha((w_{i,j}-\lambda)/\lambda)-\mu]^2}{2\sigma^2}}). \tag{8}$$

The first derivative of $f(new_x)$ is:

$$f'(new_x) = 1 + \frac{2x\alpha^2}{e^{\alpha^2 x^2}}. \tag{9}$$

When $\alpha \in R$, $f'(new_x) > 0$. Similarly, when $x < -\lambda$, $f'(new_x) > 0$.

When $-\lambda \le x \le \lambda$

$$f'(new_x) \equiv 0. \tag{10}$$

Therefore, $f(new_x)$, a monofonically increasing function, is proofed.

Theorem 3. Differentiability: $f(new_x)$ is differentiable.

Proof. Because the new function is continuous and monofonically, also its right and left limit are equal. Thus, it is differentiable.

3.2. **Improved threshold parameter λ.** Completely, parameter λ plays an important role in wavelet threshold function. Ye [18] proposed a common threshold formula:

$$\lambda = \varepsilon\sqrt{2\log(N)}. \tag{11}$$

Where ε and N are noise variance and signal's sampling length respectively.

Through analyzing multiple wavelet decomposition for image, the amplitude of noise becomes smaller with the increasing of image layer. However, the amplitude of image information becomes bigger. Therefore, this paper proposes an optimized threshold parameter λ as shown in (12):

$$\lambda = \varepsilon\sqrt{2\log(N)}/\log(1+e^j). \tag{12}$$

Where j denotes the layer of image decomposition. In this formula, it can be seen that if j is increasing, the optimized λ is gradually decreased. The improved λ is superior to that in [16]. For example, when $N = 30$, $\varepsilon = 0.6$, $j = 5$, $\lambda_{[21]} = 1.5649$, our $\lambda_{new} = 0.3126$, which is a good choice for new wavelet threshold function.

Then we study the effect of j on new wavelet threshold function. Supposing $N = 30$, $\varepsilon = 0.6$. Figure 2 shows the difference, when $j = 2$, $j = 3$, $j = 5$. When j is bigger, the influence of α is very small, which can reduce noise turbulence. So our new function is effective.

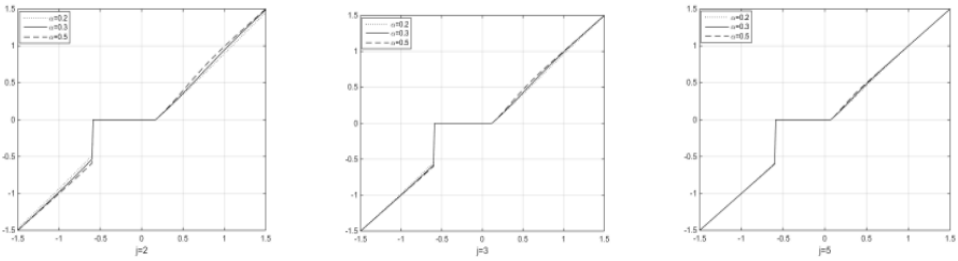

FIGURE 2. Comparison of new function with $j = 2, 3, 5$.

4. **Experiments and results.** In this section, experiments are conducted to demonstrate the effectiveness of the new threshold function with MATLAB R2014b, Core i7 CPU, 8 GB memory and Windows 10 platform. In section 4.1, evaluation criterion for our new method are introduced. Section 4.2 studies the effect of different parameters on new function for image de-noising. Section 4.3 makes comparison with state-of-the-art threshold functions to verify the effectiveness of our new method. All the experiments are conducted on the same software, hardware and laptop.

4.1. **Evaluation criterion.** In this subsection, we mainly evaluate the new function with objective evaluation. In the new function, shape parameter is adjusted to improve the influence on image de-noising. Two indicators used widely are employed to indicate the effect of image de-noising including signal-to-noise-ratio (SNR) and MSE. Considering SNR can accurately reflect the deviation between the reconstructed image and the original image, we adopt SNR as evaluation criterion:

$$SNR = 10\lg\frac{\sum_{k=1}^{N} S(k)^2}{\sum_{k=1}^{N}[X(k)-S(k)]^2}. \tag{13}$$

In this formula, N is the length of signal. $X(k)$ and $S(k)$ are noisy and original signal respectively. According to the value of SNR, we could conclude a range of shape parameter (or its fixed value) playing a better influence on image de-noising.

4.2. **Performance evaluation of different parameters for image de-noising.** Traditionally, shape parameter has a big effect on image de-noising. Thus, the selection of shape parameter is very important.

According to the principle of Gaussian kernel function, α is with a better curve. First, we study the effect of μ and σ on the image de-noising. Assuming that $N = 30$, $\varepsilon = 0.6$, $j = 0.2$. In actual experiments process, 785 images are to test the performance of the algorithm. Because this paper space is limited, we only select "Lena, Barbara, Baboon" in international standard test images as the testing data shown in Figure3.

FIGURE 3. Original images. (a) Lena; (b) Barbara; (c) Baboon. Noisy images. (c) Lena; (d) Barbara; (e) Baboon.

Meanwhile, Tables 1-3 are the SNRs (better results with Bold Font) with different σ and μ to deeply illustrate the effectiveness of our method. Where SNR1 and SNR2 denote the signal-to-noise ratio of original image and de-noising image respectively.

TABLE 1. SNR value of Lena with different σ and μ.

Number	Parameter	SNR1	SNR2
1	$\sigma_1^2 = 0.1$, $\mu_1 = 0$	14.3802	21.7439
2	$\sigma_2^2 = 0.3$, $\mu_1 = 0$	14.4087	21.1119
3	$\sigma_3^2 = 0.6$, $\mu_1 = 0$	14.3965	20.5175
4	$\sigma_1^2 = 0.1$, $\mu_1 = 2$	14.4273	21.4741
5	$\sigma_2^2 = 0.3$, $\mu_1 = 2$	14.4174	19.5411
6	$\sigma_3^2 = 0.6$, $\mu_1 = 2$	14.4080	18.5556
7	$\sigma_1^2 = 0.1$, $\mu_1 = 5$	14.4138	18.6694
8	$\sigma_2^2 = 0.3$, $\mu_1 = 5$	14.4074	21.0585
9	$\sigma_3^2 = 0.6$, $\mu_1 = 5$	14.4049	19.7357

To explore the influence of each parameter, we choose different values of σ and μ to discuss. We conduct experiments on Lena, Barbara and Baboon. The noise we use

TABLE 2. SNR value of Barbara with different σ and μ.

Number	Parameter	SNR1	SNR2
1	$\sigma_1^2 = 0.1$, $\mu_1 = 0$	13.6973	17.2129
2	$\sigma_2^2 = 0.3$, $\mu_1 = 0$	13.6909	17.0624
3	$\sigma_3^2 = 0.6$, $\mu_1 = 0$	13.6843	17.0355
4	$\sigma_1^2 = 0.1$, $\mu_1 = 2$	13.6792	17.1461
5	$\sigma_2^2 = 0.3$, $\mu_1 = 2$	13.6664	17.0439
6	$\sigma_3^2 = 0.6$, $\mu_1 = 2$	13.6779	17.1425
7	$\sigma_1^2 = 0.1$, $\mu_1 = 5$	13.6768	16.9140
8	$\sigma_2^2 = 0.3$, $\mu_1 = 5$	13.6958	16.8567
9	$\sigma_3^2 = 0.6$, $\mu_1 = 5$	13.6625	16.1687

TABLE 3. SNR value of Baboon with different σ and μ.

Number	Parameter	SNR1	SNR2
1	$\sigma_1^2 = 0.1$, $\mu_1 = 0$	14.5849	15.8694
2	$\sigma_2^2 = 0.3$, $\mu_1 = 0$	14.5648	15.8683
3	$\sigma_3^2 = 0.6$, $\mu_1 = 0$	14.5765	15.2038
4	$\sigma_1^2 = 0.1$, $\mu_1 = 2$	14.5691	15.2581
5	$\sigma_2^2 = 0.3$, $\mu_1 = 2$	14.6053	15.0424
6	$\sigma_3^2 = 0.6$, $\mu_1 = 2$	14.5698	15.6188
7	$\sigma_1^2 = 0.1$, $\mu_1 = 5$	14.5696	14.7447
8	$\sigma_2^2 = 0.3$, $\mu_1 = 5$	14.5739	15.5586
9	$\sigma_3^2 = 0.6$, $\mu_1 = 5$	14.5721	15.1356

is predominantly normal Gaussian noise 0.01. We list the de-noising results of Lena, Barbara and Baboon as Tables 1-3, different SNRs are obtained. From Table 1, we can know that if σ and μ are selected different values, SNRs of image with new threshold function are different. When $\sigma_2^2 = 0.1$, $\mu_1 = 0$, SNR2 is 21.7439 exceeding the value that when $\sigma_2^2 = 0.3$ and $\mu_2 = 5$. Similarly, when $\sigma_2^2 = 0.1$, $\mu_2 = 2$, the SNR2 is the biggest with 21.4741 than $\sigma_2^2 = 0.3$ and $\sigma_2^2 = 0.6$ with 19.5411 and 18.5556 respectively. Furthermore, when $\mu_2 = 0$ and $\mu_2 = 2$, the average value of SNR is bigger than $\mu_2 = 5$. When $\sigma_2^2 = 0.1$, $\mu_2 = 0$, the value of SNR is 21.7439 over the value when $\sigma_2^2 = 0.1$, $\mu_2 = 2$ with 21.4741. Similarly, the results are better with our method presented in table 2 and table 3.

4.3. **Discussion for parameter ε.** Through the above analysis on μ, σ, j, let $\mu = 0$, $j = 5$, $\sigma_1^2 = 0.1$, $N = 30$ and $\alpha = 1$ in this subsection. We make six experiments to study the effect of shape parameter ε on the image de-noising for Lena, Barbara and Baboon. Results are listed in tables 4-6.

TABLE 4. SNR value of Lena with different ε.

Number	Parameter	SNR1	SNR2
1	$\varepsilon_1 = 0.1$	14.3957	21.8106
2	$\varepsilon_1 = 0.2$	14.3677	21.5676
3	$\varepsilon_1 = 0.4$	14.4052	21.5144
4	$\varepsilon_1 = 0.6$	14.4083	21.3922
5	$\varepsilon_1 = 0.8$	14.4200	20.9781
6	$\varepsilon_1 = 0.9$	19.9188	14.4240

Table 5. SNR value of Barbara with different ε.

Number	Parameter	SNR1	SNR2
1	$\varepsilon_1 = 0.1$	13.6689	17.3208
2	$\varepsilon_1 = 0.2$	13.6811	17.2746
3	$\varepsilon_1 = 0.4$	13.6825	17.1159
4	$\varepsilon_1 = 0.6$	13.6797	17.1400
5	$\varepsilon_1 = 0.8$	13.6728	17.1285
6	$\varepsilon_1 = 0.9$	13.6926	16.5752

Table 6. SNR value of Barboon with different ε.

Number	Parameter	SNR1	SNR2
1	$\varepsilon_1 = 0.1$	14.5826	16.0097
2	$\varepsilon_1 = 0.2$	14.5654	15.8767
3	$\varepsilon_1 = 0.4$	14.5916	15.4120
4	$\varepsilon_1 = 0.6$	14.5698	15.3762
5	$\varepsilon_1 = 0.8$	14.5647	15.0478
6	$\varepsilon_1 = 0.9$	14.5934	14.9780

4.4. **Comparison experiments.** In our experiments, we compare the performances of six different algorithms: soft threshold function, Lu [19], Han [20], Li [21], Srivastava [22] and the proposed method. In order to demonstrate the comparison fairness, the parameters are set as $\mu = 0$, $j = 5$, $\sigma_1^2 = 0.1$, $N = 30$, $\varepsilon = 0.1$ and $\alpha = 1$ due to the familiar de-noising model.

We repeat the experimental process 30 times. The performances of different algorithms are measured quantitatively using SNR. Figures 4-6 give the de-noising results of different algorithms for Lena, Barbara and Baboon. Tables 7-9 list de-noising results of different methods in terms of SNR and SSIM (structural similarity). From these tables we can see that our algorithm outperforms the traditional soft threshold function and the method in [16-19] in the same Gaussian noise. The result of our algorithm is slight better than those in [19-22] in quantitative comparison. In each such we highlighted the best result. From the discussion above, we know that our new method has a good performance and better than these state-of-art techniques in most situations.

Table 7. SNR comparison of Lena with different methods.

Method	Soft	Lu	Han	Li	Srivastava	New
SNR1	14.4317	14.4201	14.3878	14.4261	14.3962	14.3978
SNR2	20.3449	20.7895	21.5429	20.6744	21.7421	22.6259
SSIM	0.8052	0.8419	0.8758	0.9173	0.9451	0.9746

Table 8. SNR comparison of Barbara with different methods.

Method	Soft	Lu	Han	Li	Srivastava	New
SNR1	14.5844	13.6808	13.6706	13.6807	13.6851	13.6923
SNR2	14.8547	16.1256	17.3611	16.6059	16.2282	17.4083
SSIM	0.7935	0.8152	0.8466	0.8793	0.9258	0.9477

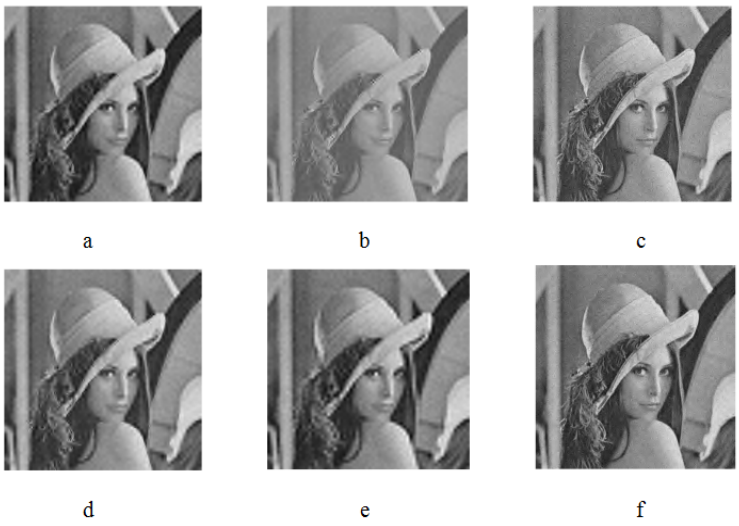

FIGURE 4. Lena comparison of New Method with other de-noising methods. (a) De-noising with Soft threshold function; (b) Lu method; (c) Han method; (d) Li method; (e) Srivastava method; (f) Our new method.

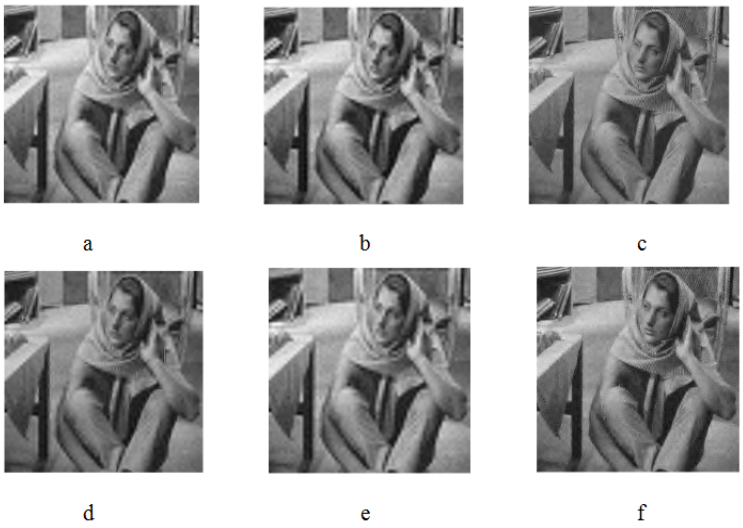

FIGURE 5. Barbara comparison of New Method with other de-noising methods. (a) De-noising with Soft threshold function; (b) Lu method; (c) Han method; (d) Li method; (e) Srivastava method; (f) Our new method.

TABLE 9. SNR comparison of Baboon with different methods.

Method	Soft	Lu	Han	Li	Srivastava	New
SNR1	14.4316	14.5606	14.6007	14.5647	14.3862	14.5739
SNR2	14.8547	14.8330	16.0908	15.8385	15.4820	17.2237
SSIM	0.8579	0.8861	0.9214	0.9357	0.9411	0.9652

According to table 7, SNR2 21.6419 of our new method is the biggest value among all the functions, then next is Srivastava method with 21.7421, followed by Han method, reaching to 21.5429; and finally come Lu method, Li method, soft threshold function at 20.7895, 20.6744 and 20.3449 respectively. Overall, what is noticeable from the table is

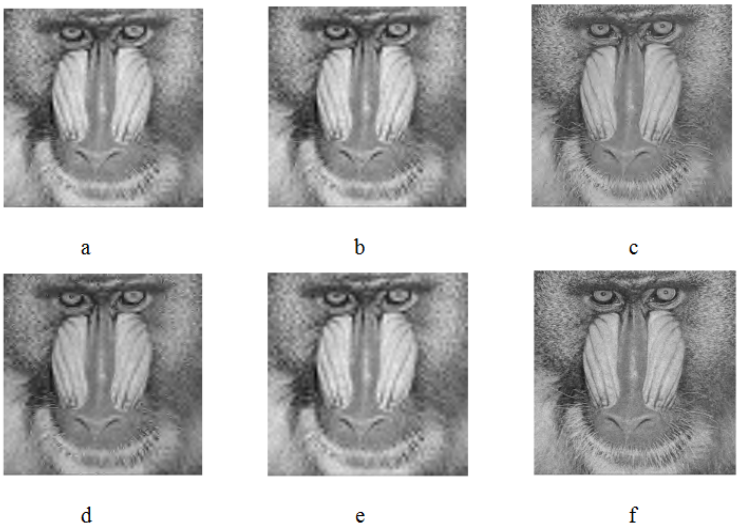

FIGURE 6. Baboon comparison of New Method with other de-noising methods. (a) De-noising with Soft threshold function; (b) Lu method; (c) Han method; (d) Li method; (e) Srivastava method; (f) Our new method.

that our new method has better effect, similarly as presented in tables 8,9. There are some spots in soft threshold function. Lu method indicates that the de-noising effect has better smooth, but the image is fuzzy. In these test images, similarity among neighboring blocks is easy to perceive in the uniform regions and along the regular-shaped structures. The de-noising performance of new algorithm is highlighted. We find that various image details are well preserved and at the same time very few artifacts are introduced with new method. The computation time is given in table 10. From the table, we can know that the proposed method only takes approximately 1.36s, 1.38s and 1.39s for Lena, Barbara and Baboon respectively, which is better than other methods.

TABLE 10. Computation time comparison with different methods(s).

Method	Soft	Lu	Han	Li	Srivastava	New
Lena	1.68	1.74	1.65	1.59	1.61	1.36
Barbara	1.66	1.73	1.61	1.58	1.58	1.38
Baboon	1.72	1.75	1.66	1.62	1.53	1.39

5. **Conclusions.** This paper proposed a new wavelet threshold function based on Gaussian kernel function for image de-noising for the first time. The new idea was embedded in two aspects: introducing Gaussian kernel function into soft threshold function; improving the shape parameter λ. In this paper, we detailed discussed our new function including the relation between j and α, effect of ε. Furthermore, the proof was given to demonstrate its good properties. Finally, experiments were conducted to show the good effect of our method. It could be clearly seen that image de-noising with new wavelet threshold function was more closely to original image. To be more special, the new method made up some demerits in recent threshold functions and it could achieve effective de-noising results.

Acknowledgement. This work is supported by the Natural Science Fund Guiding Program in Liaoning Province (Grant No.20180520024).

REFERENCES

[1] J. S. Pan, J. B. Li, Z. M. Lu, Adaptive quasiconformal kernel discriminant analysis, *[J]. Neurocomputing,* vol. 71. no. 13, pp. 2754-2760, 2008.

[2] J. B. Li, M. Li, J. S. Pan, et al. Gabor-based kernel self-optimization Fisher discriminant for optical character segmentation from text-image-mixed document, *Journal of. Optik - International Journal for Light and Electron Optics*, vol. 126, no. 21, pp. 3119-3124, 2015.

[3] X. Y. Chen, X. Y. Peng, J. B. Li, and Y. Peng, Overview of Deep Kernel Learning Based Techniques and Applications, *Journal of Network Intelligence*, vol. 1, no. 3, pp. 82-97, Aug 2016

[4] Y. Ji, D. Li, M. Yu, et al. A de-noising algorithm based on wavelet threshold-exponential adaptive window width-fitting for ground electrical source airborne transient electromagnetic signal, *Journal of. Journal of Applied Geophysics.*; vol. 128, pp. 1-7 2016.

[5] J. B. Li , J. S. Pan , Z. M. Lu, Kernel optimization-based discriminant analysis for face recognition, *Journal of Neural Computing & Applications*, vol. 18, no. 6, pp. 603-612, 2009.

[6] D. L. Donoho, J. M. Johnstone, Ideal spatial adaptation by wavelet shrinkage. Biometrika, vol. 81, no. 3, pp. 425-455, 1994.

[7] S. Xie, T. Xu, X. Han, et al. Accuracy improvement of quantitative LIBS analysis using wavelet threshold de-noising, *Journal of Analytical Atomic Spectrometry.* 2017.

[8] M. Bachmayr , R. Schneider Iterative Methods Based on Soft Thresholding of Hierarchical Tensors. *Foundations of Computational Mathematics;* pp. 1-47, 2016.

[9] Mcginnity K, Varbanov R, Chicken E. Cross-validated wavelet block thresholding for non-Gaussian errors. Computational Statistics & Data Analysis. 2017; 106:127-137.

[10] A. K. Bhandari ,A. Kumar , Singh G K, et al. Performance study of evolutionary algorithm for different wavelet filters for satellite image denoising using sub-band adaptive threshold. *Journal of Experimental & Theoretical Artificial Intelligence*, vol. 28, no. (1-2), pp. 71-95, 2016.

[11] S. Sulochana, R. Vidhya, D. Vijayasekaran , et al. Denoising and Dimensionality Reduction of Hyperspectral Images Using Framelet Transform with Different Shrinkage Functions, vol. 45, no. 8, pp. 978-986, pp. 2016.

[12] Q. Wang , H. Wen, Y. Han , et al. The research and application of image de-noising based on the improved method of wavelet thresholding[C]// International Conference on Intelligent Earth Observing and Applications. 2015:98083U.

[13] S. A. Kadhim. A New Signal De-Noising Method Using Adaptive Wavelet Threshold based on PSO Algorithm and Kurtosis Measuring for Residual Noise. Journal of Babylon University; vol. 25, no. 1, pp. 8-19. 2017.

[14] Y. Ji , D. Li, M. Yu , et al. A de-noising algorithm based on wavelet threshold-exponential adaptive window width-fitting for ground electrical source airborne transient electromagnetic signal. Journal of Applied Geophysics, vol. 128, pp. 1-7.

[15] Ke D, Z. Lu , Luo M K. A Denoising Algorithm for Noisy Chaotic Signals Based on the Higher Order Threshold Function in Wavelet-Packet. *Chinese Physics Letters.* vol. 28, no. 2, pp. 0205-0215, 2011

[16] Y. Kim , Oh C, Sohn K. Edge-aware image smoothing using commute time distances*[C]// IEEE International Conference on Image Processing. IEEE,* 2016, pp. 3304-3308.

[17] R. Averkamp, C. Houdr Wavelet Thresholding for Non-Necessarily Gaussian Noise: Idealism. *Annals of Statistics.* 2006, vol 31, no. 1, pp.110-151.

[18] J. Ye Using an improved measure function of vague sets for multicriteria fuzzy decision-making. *Expert Systems with Applications: An International Journal.*2010; vol. 37, no. 6, pp.4706-4709.

[19] J. Y. Lu , L. Hong, Y. Dong , et al. A New Wavelet Threshold Function and Denoising Application. Mathematical Problems in Engineering. 2016; vol. 2016, no. 3, pp.1-8.

[20] G. Han, Z. Xu Electrocardiogram signal denoising based on a new improved wavelet thresholding. *Review of Scientific Instruments*, vol. 87, no. 8, p.7432-1294, 2016.

[21] H. Li, C. Y. Suen A novel Non-local means image denoising method based on grey theory. *Pattern Recognition.* 2016;vol. 49, pp. 237-248.

[22] M. Srivastava, C. L. Anderson, J. H. Freed A New Wavelet Denoising Method for Selecting Decomposition Levels and Noise Thresholds. *IEEE Access Practical Innovations Open Solutions* ; vol. 4, vol. 38-62, 2016.